Radiation Patterns of a Noise-Excited Thin Slot*

NICHOLAS GEORGE†, MEMBER, IRE

Summary—Theoretical and experimental radiation patterns are given in spectral form for the thermal radiation from a cylindrical discharge column which is adjacent to a long thin slot in a metallic plane. A spatial distribution is predicted which exhibits interference minima and maxima when the length of the slot and the wavelength of the emission are the same order of magnitude. The analysis is based on Maxwell's equations and the Leontovich-Rytov distributed source generalization of Nyquist's noise formula.

Fraunhofer pattern measurements are presented in which an argon source is used to excite slots of 7.3π and 9.5π radians in length. Data are also presented to show the effects of variations in the pressure and the dc current of the discharge. The pattern measuring apparatus is a Dicke radiometer, having the following characteristics: frequency 9200 Mc, bandwidth to the detector 16 mc, modulation frequency 1000 cps, and residual noise level 0.3 rms°K.

An interference phenomenon is predicted by the theory and demonstrated by an experiment, even though the source excitation is spatially distributed and essentially uncorrelated in time and in space. The patterns are not even approximately Lambertian, *e.g.*, a thin slot of 9.5π radians exhibits a pattern having nine relative maxima in 180°, with the maximum emission at 63° from the normal.

I. Introduction

THE chaotic motion of the electrons in a plasma or in a metal gives rise to electromagnetic radiation over a wide spectrum which includes the microwave frequencies. The terminal characteristics of such noise sources have been studied both theoretically [1], [2] and experimentally [3], [4]. On the other hand, while the distributed nature of the noise arising from such sources has been recognized from the time of the earliest work in the theory of fluctuations, it had received comparatively little attention until the derivation by Leontovich and Rytov [5] of the formula for the correlation function of the noise electric field in a lossy medium, (1) below. In this paper, attention is directed to a related problem, an analysis and an experiment, in which the distributed nature of the noise plays a dominant role. Specifically, the problem is to determine the far-zone radiation pattern for a long thin slot which is excited by a distributed noise source.

In the analysis which follows it is necessary to use the distributed source description derived by Leontovich and Rytov. Their formula for the correlation function of the x component of the effective noise electric field in a conductive medium is given by

$$\langle E_x(\boldsymbol{r}, t)E_x^*(\boldsymbol{r} - \boldsymbol{r}_0, t - t_0)\rangle = \frac{2\bar{\epsilon}}{\sigma}\delta(r_0)\delta(t_0). \tag{1}$$

If a generalized Ohm's law holds for the medium, *i.e.*, if $j(r) = \sigma E(r)$, then an equivalent expression for the correlation function of the x component of the current density is given by

$$\langle j_x(\boldsymbol{r}, t)j_x^*(\boldsymbol{r} - \boldsymbol{r}_0, t - t_0)\rangle = 2\bar{\epsilon}\sigma\delta(r_0)\delta(t_0). \tag{2}$$

$E_x(\boldsymbol{r}, t)$ and $j_x(\boldsymbol{r}, t)$ are the x components of the source electric field and the current density, respectively; $\delta(\boldsymbol{r})$ is Dirac's delta function; σ is the conductivity; and $\bar{\epsilon}$ is the mean energy per degree of freedom given by Planck as

$$\bar{\epsilon} = \frac{hf}{e^{hf/kT} - 1}, \tag{3}$$

where f is the frequency, T is the absolute temperature, h is Planck's constant, and k is the Boltzmann constant.

The angular parentheses, $\langle\ \rangle$, are used throughout this paper to denote an ensemble average. A second notational convenience, adopted herein, is that time dependence is always indicated explicitly while frequency dependence is not. Therefore, $E(x, y)$ may mean $E(x, y, \omega)$, but it will never mean $E(x, y, t)$.

An important result in spectral analysis is quoted for later use. Let $f(x, t)$ be a sample function of a stationary random process. It can be shown that the two-dimensional correlation function, and the mixed spectral density and correlation function, satisfy the following Fourier transform relationship.

$$\int_{-\infty}^{\infty}\langle f(x_1, t)f^*(x_2, t - t_0)\rangle e^{-i\omega t_0}dt_0 = \lim_{2T\to\infty}\left\langle\frac{F(x_1, \omega)F^*(x_2, \omega)}{2T}\right\rangle \tag{4}$$

in which

$$F(x, \omega) = \int_{-T}^{T} f(x, t)e^{-i\omega t}dt.$$

II. Theoretical Radiation Patterns

Consider a metallic plate in the $y=0$ plane with a long thin z-oriented aperture of dimensions (a, b) where $a \gg b$ (Fig. 1). The aperture is illuminated or excited by a distributed noise source that generates electromagnetic energy which is incoherent spatially and timewise, *e.g.*, a closely-spaced hot wire or a plasma column (Section III). An approximate analysis for the resultant aperture distribution is made in the following section. The effects of radiation losses are neglected; and furthermore, aside from the generation of the noise, the influence of the noise medium of contrasting dielectric constant and

* Received by the PGMTT, January 28, 1960; revised manuscript received, May 16, 1960.

† Calif. Inst. Tech., Pasadena, Calif. Formerly with Engrg. Div., Hughes Aircraft Co, Culver City, Calif.

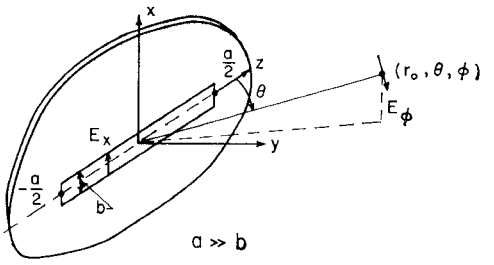

Fig. 1—Coordinates for the thin slot.

conductivity is assumed calculable, by allowing for a perturbation in the propagation constant for the region surrounding the slot.

A. Approximate Aperture Illumination for the Thin Slot

A simple transmission line model is used below in order to obtain an approximate expression for the resultant electric field, which is induced in the aperture by the distributed noise source. For this transmission line model, it is convenient to express the noise excitation in terms of a distributed source current that is induced in the metallic plane by the rapidly moving plasma electrons (Fig. 2). An approximate value for this current is obtained in the following manner. Let the noise source, rapidly moving plasma electrons, fill the half-space for which $y<0$, and suppose that the plate at $y=0$ is not slotted. The moving electrons induce eddy currents; but over the range of frequencies for which the plasma is opaque, only those electrons close to the plate are effective in inducing these currents. It is assumed that the characteristic depth is the absorption skin depth of the plasma, δ. Let $I_s(x, z, \omega)$ be the x component of the induced eddy current measured in units of current per unit frequency interval per unit length in the z direction and let $I_s(z, \omega)$ be the x component of this surface current averaged over a length b which corresponds to the narrow dimension of the slot, *i.e.*,

$$I_s(z, \omega) = \frac{1}{b}\int_{-b/2}^{b/2} I_s(x, z, \omega)dx.$$

This surface current can be expressed in terms of the x component of the noise current density, $j_x(x, y, z, \omega)$, by

$$I_s(z, \omega) \approx \frac{1}{b}\int_{-\delta}^{0}\int_{-b/2}^{b/2} j_x(x, y, z, \omega)dxdy, \qquad (5)$$

where j_x is measured in units of current per unit frequency interval per unit area in the y-z plane. The integrations are required in order to take account of the spatial incoherence of the noise currents. Eqs. (2), (4), (5) are combined to give the following mixed spectral density and correlation function for the x component of the source current in the metal plate.

$$\lim_{2T\to\infty}\left\langle\frac{I_s(z_1, \omega)I_s^*(z_2, \omega)}{2T}\right\rangle = \frac{2\bar{\epsilon}\sigma\delta}{b}\delta(z_1 - z_2). \qquad (6)$$

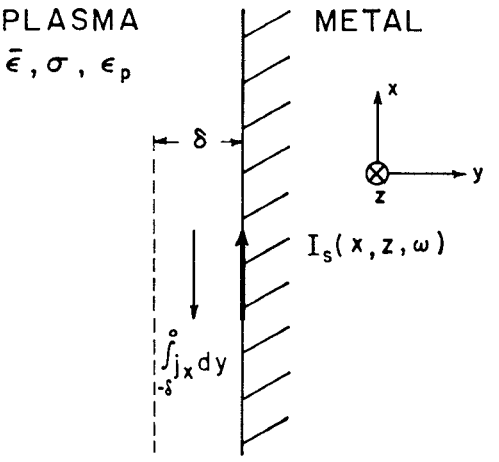

Fig. 2—Induced current approximation.

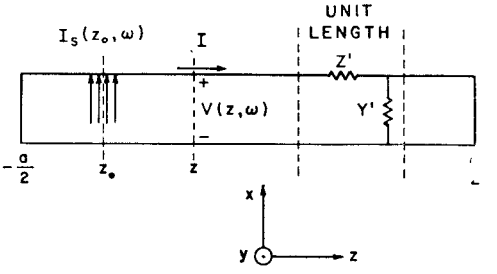

Fig. 3—Transmission-line model for the aperture distribution of the electric field.

Now with a slotted plane, the influence of the source current, I_s, in the region from z to $z+dz$ is felt everywhere along the gap. Consider the principal mode analysis in which the slot is viewed as a transmission line with the source field propagating mainly along the gap and with a standing wave being established by the reflections at $z=\pm a/2$ (Fig. 3). The voltage per unit frequency interval, V, and the current per unit frequency interval, I, are related in the following manner by the transmission line equations:

$$\frac{\partial V}{\partial z} = -Z'I \qquad (7)$$

and

$$\frac{\partial I}{\partial z} = -Y'V + I_s(z, \omega), \qquad (8)$$

where the series impedance per unit length, Z', and the shunt admittance per unit length, Y', are related to the complex propagation factor, $\beta_c=\beta-i\alpha$, by

$$\beta_c^2 = -Y'Z' \qquad (9)$$

and where the potential, V, is defined by

$$V = \int_{-b/2}^{b/2} E_x(x, 0, z, \omega)dx.$$

Taking $\partial/\partial z$ of (7) and substituting from (8), (9) give the wave equation for V,

$$\frac{\partial^2 V}{\partial z^2} + \beta_c^2 V = -Z' I_s(z, \omega). \tag{10}$$

The general solution of (10), subject to the boundary condition that $V(\pm a/2, \omega) = 0$, is readily obtained by standard methods; and the result is given by

$$V(z, \omega) = \int_{-a/2}^{+a/2} Z' I_s(z_0, \omega) \frac{1}{2\beta_c} \cdot \left[\frac{\cos \beta_c(z + z_0) - \cos \beta_c(a - |z - z_0|)}{\sin \beta_c a}\right] dz_0 \tag{11}$$

where an alternative special form must be written for the cases in which $\beta_c a = \pi, 2\pi, 3\pi, \cdots$.

In the final result, an expression containing Z' is not convenient. This series impedance per unit length can be eliminated in favor of a more fundamental impedance parameter by means of an approximate relation developed in (14) below. Using the form of Babinet's principle as generalized for vector fields by Booker [6], [7], one can readily establish the following relationship between Z', Y' for a slot and the corresponding Z'', Y'' for the complementary electric dipole, *i.e.*, a thin metallic strip of cross section a by b.

$$\frac{Z'}{Y''} = \frac{\eta^2}{2} \quad \text{and} \quad \frac{Y'}{Z''} = \frac{2}{\eta^2}, \tag{12}$$

where η is the characteristic impedance for the medium which surrounds the antenna. Then, using the transmission line model for the *metallic* dipole and expressing the input impedance of a center-driven antenna in terms of an open-circuited line of length $a/2$, one obtains

$$Y'' = \frac{\beta_c \cot \frac{\beta_c a}{2}}{z_{in}}, \tag{13}$$

in which z_{in} is the input impedance of the center-driven *metallic* dipole of length a. Strictly, the admittance per unit length varies along the length of the antenna; hence, (13) should be regarded as a defining equation for an averaged admittance to be used with the transmission line model.[1] Combining (12) and (13), one obtains the final expression for the Z' of the slot, *i.e.*,

$$Z' = \frac{\eta^2 \beta_c \cot \frac{\beta_c a}{2}}{2 z_{in}}. \tag{14}$$

[1] The result in (13) can also be deduced in another, perhaps more fundamental, way from (19), (24), (25) of Weber [8].

Elimination of Z' in (11) by (14) gives the following result for the aperature illumination:

$$V(z, \omega) = \frac{\eta^2}{4 z_{in}} \int_{-a/2}^{a/2} I_s(z_0, \omega) \cdot \left[\frac{\cos \beta_c(z + z_0) - \cos \beta_c(a - |z - z_0|)}{1 - \cos \beta_c a}\right] dz_0. \tag{15}$$

B. Radiation in the Fraunhofer Region

The approximate tangential electric field over the $y = 0$ plane is now determined. The specification of the tangential electric field over this plane together with the radiation condition for the field as $r_0 \to \infty$ are sufficient to uniquely determine the radiation field. The radiation field is conveniently expressed in terms of the Fourier integral analog of (1-14.19) of Smythe [9]. This formula gives the exact diffracted vector potential, $\boldsymbol{A}$, in terms of the aperture distribution for an arbitrary aperture. Differentiating, since $\boldsymbol{E} = -\partial \boldsymbol{A}/\partial t$, suppressing the $e^{i\omega t}$ factor, dropping the near-zone term, and making the usual far-zone approximation in the phase term, *i.e.*, $r \approx r_0 - z_1 \cos \theta$, one can reduce (1-14.19) to the following form:

$$E_\phi(r_0, \theta, \phi, \omega) = \frac{-i\beta_0 \sin \theta e^{-i\beta_0 r_0}}{2\pi r_0} \int_{-a/2}^{a/2} V(z, \omega) e^{i\beta_0 z \cos \theta} dz, \tag{16}$$

in which the coordinates (r_0, θ, ϕ) are the radius, the polar angle, and the azimuthal angle measured in the x-y plane from the x axis. (See Fig. 1.)

In the far-zone, the power radiated through a solid angle $d\Omega$ is given by Poynting's theorem as the product $[r_0 E_\phi(r_0, \theta, \phi, t)]^2 d\Omega/\eta$. From this, it follows that in spectral form, the average power radiated through a solid angle $d\Omega$ in the frequency interval df is given by

$$P_{f\Omega} df d\Omega = \lim_{2T \to \infty} \frac{2 r_0^2}{\eta} \left\langle \frac{E_\phi(r_0, \theta, \phi, \omega) E_\phi^*(r_0, \theta, \phi, \omega)}{2T} \right\rangle df d\Omega. \tag{17}$$

Arbitrarily, the power through a unit solid angle per unit frequency interval, $P_{f\Omega}$, is defined above on the basis of a one-sided frequency interval, *i.e.*, the total average power per solid angle is given by $\int_0^\infty P_{f\Omega} df$. Substitution of (15), (16) into (17) gives the following integral form for the radiation pattern of the slot:

$$P_{f\Omega} = \frac{\eta}{8\pi^2} \left[\frac{\eta |\beta_c| \sin \theta}{|z_{in}| \beta_0}\right]^2 \int_{-a/2}^{a/2} \int_{-a/2}^{a/2} \int_{-a/2}^{a/2} \int_{-a/2}^{a/2} \times \lim_{T \to \infty} \left\langle \frac{I_s(z_0, \omega) I_s^*(z_1, \omega)}{2T} \right\rangle \times \left[\frac{\cos \beta_c(z_2 + z_0) - \cos \beta_c(a - |z_2 - z_0|)}{2\beta_c(1 - \cos \beta_c a)}\right] \times \left[\frac{\cos \beta_c(z_3 + z_1) - \cos \beta_c(a - |z_3 - z_1|)}{2\beta_c(1 - \cos \beta_c a)}\right]^* \times e^{i\beta_0(z_2 - z_3)\cos \theta} \beta_0^4 dz_0 dz_1 dz_2 dz_3. \tag{18}$$

C. Radiation Pattern for the Delta-Correlated Source

Eq. (18) is integrated directly with respect to the variables z_2 and z_3. Then, (6) is substituted for the source function, and the expression is integrated with respect to z_0 and z_1. These integrations lead in a tedious but straightforward way to the intermediate form given below.

$$P_{f\Omega} = \frac{\eta\bar{\epsilon}\sigma\delta}{4\pi^2 b}\left[\frac{\eta\,|\,\beta_c\,|}{|\,z_{in}\,|\,\beta_0}\right]^2 \cdot \frac{4\beta_0^4 \sin^2\theta}{|\,1-\cos\beta_c a\,|^2\,|\,\beta_c^2-(\beta_0\cos\theta)^2\,|^2} K_1, \tag{19}$$

in which

$$K_1 = a\left|\sin\beta_c\frac{a}{2}\cos\beta_c\frac{a}{2}\right|^2 + \frac{\sinh\alpha a}{2\alpha}\left[\left|\sin\beta_c\frac{a}{2}\right|^2\cos^2\left(\beta_0\frac{a}{2}\cos\theta\right) + \left|\cos\beta_c\frac{a}{2}\right|^2\sin^2\left(\beta_0\frac{a}{2}\cos\theta\right)\right] + \frac{\sin\beta a}{2\beta}\left[\left|\sin\beta_c\frac{a}{2}\right|^2\cos^2\left(\beta_0\frac{a}{2}\cos\theta\right) - \left|\cos\beta_c\frac{a}{2}\right|^2\sin^2\left(\beta_0\frac{a}{2}\cos\theta\right)\right] + \mathrm{Re}\frac{\beta_c^*\sin\beta_c a}{\beta_c^{*2}-(\beta_0\cos\theta)^2}\left[\cos\beta_c^* a-\cos(\beta_0 a\cos\theta)\right].$$

Eq. (19) is not in a convenient form for computation. A more convenient form is obtained by introducing a $(4\beta_0)$ portion of the coefficient into the central bracket, replacing β_0/η by $\omega\epsilon_0$, and eliminating β_c in favor of α, β. Finally, after considerable manipulation, the following expression is obtained for the one-sided spectral intensity of the power which is radiated per unit frequency per unit solid angle:

$$P_{f\Omega} = \frac{\sigma\delta\bar{\epsilon}\eta^2(\rho^2+\gamma^2)(\sin\theta)^2 K_2}{4\pi^2\omega\epsilon_0 b\,|\,z_{in}\,|^2[\cosh\alpha a-\cos\beta a]^2[(\gamma^2-\rho^2-\cos^2\theta)^2+4(\gamma\rho)^2]} \tag{20}$$

in which

$$K_2 = \beta_0 a\left\{\frac{\sinh\alpha a}{\alpha a}\left[\cosh\alpha a-\cos(\beta_0 a\cos\theta)\cos\beta a\right] + \frac{1}{2}\cosh 2\alpha a-\frac{1}{2}\cos 2\beta a\right\} + \frac{\beta_0\sin\beta a}{\beta}\left[-\cos\beta a+\cos(\beta_0 a\cos\theta)\cosh\alpha a\right] + \frac{4}{(\gamma^2-\rho^2-\cos^2\theta)^2+4(\gamma\rho)^2}\{\gamma[\gamma^2+\rho^2-\cos^2\theta] \times\sin\beta a[\cos\beta a-\cos(\beta_0 a\cos\theta)\cosh\alpha a] - \rho[\gamma^2+\rho^2+\cos^2\theta]\sinh\alpha a \times[\cosh\alpha a-\cos(\beta_0 a\cos\theta)\cos\beta a]\}$$

and where

a = length of the slot (Fig. 1),
b = width of the slot, $b\ll\lambda$,
$\sigma\delta$ = conductivity, skin-depth product for the plasma,
$i\beta_c = i\beta+\alpha$,
$\gamma = \beta/\beta_0$,
$\rho = \alpha/\beta_0$,
z_{in} = input impedance of center-driven complementary metallic dipole [7],
$\eta = (\mu_0/\epsilon_0)^{1/2} \cong 377$ ohms,
$\omega = 2\pi f$.

The above equation represents a first order approximation to the radiation pattern for a thin slot which is excited incoherently both spatially and timewise. This analysis is similar to that of Levin and Rytov [10] for the thermal radiation pattern of a thin linear antenna. However, even allowing for the complementary aspect, there are two differences. First, the solution (20) appears to apply for a greater range of lengths due to the incorporation of z_{in} [11]. Secondly, a complex wave number is assumed for the propagation along the slot in order to account for loss and phase retardation due to the noise source. Setting $\alpha=0$ and $\beta=\beta_0$ in (20), one finds that the *spatial variation* agrees with that obtained by Levin and Rytov.

D. Selected Cases

Radiation patterns are plotted for several different slot lengths when there is no loss and when the wave numbers are equal (Fig. 4). The graphs are of $P_{f\Omega}$ (from (20) with $\alpha=0, \beta=\beta_0$) normalized to $\sigma\delta\bar{\epsilon}\eta^2/(4\pi^2\omega\epsilon_0 b\,|\,z_{in}\,|^2)$ and plotted vs the angle from the normal, $\pi/2-\theta$, for values of the length $\beta a/\pi = 2.5$, 4.5, 6.5, and 8.5.

Radiation patterns are also plotted for a variable loss factor but with a fixed length and with no phase retardation (Fig. 5). The graphs are of $P_{f\Omega}$ (from (20) with $\beta=\beta_0$, $\beta_0 a = 9.5\pi$) normalized to $\sigma\delta\bar{\epsilon}\eta^2/(4\pi^2\omega\epsilon_0 b\,|\,z_{in}\,|^2)$ and with the attenuation parameter, α, selected to give 0, 1, 3, 5, and 20 db of attenuation per wavelength.

III. Experimental Radiation Patterns

There are two radiation experiments which would be very interesting to perform in the course of verifying the theory. One of these is the measurement of the thermal radiation from a hot wire of moderately high conductivity. In order to make this measurement in the far zone at microwave frequencies, it has been estimated that receiver sensitivities of 2×10^{-3}°K and 0.1°K are required using sources of tungsten and silicon carbide, respectively [11]. Restricting the receiver bandwidth to approximately 100 mc in order to prevent excessive smoothing of the pattern, one concludes that

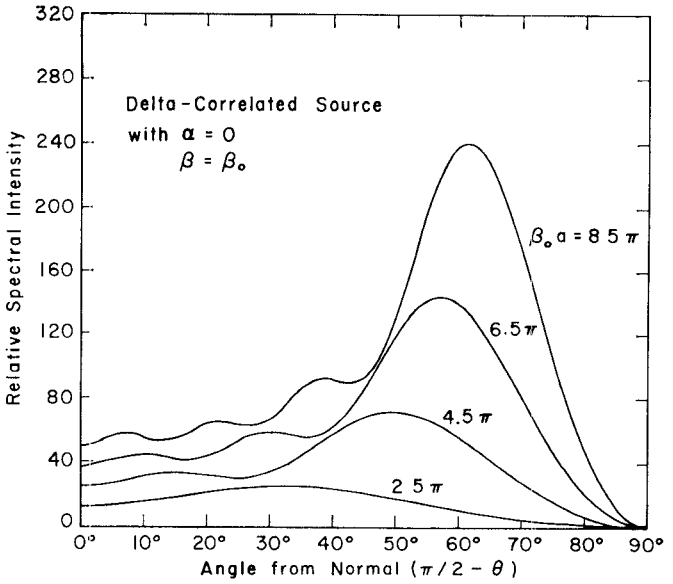

Fig. 4—Thermal radiation patterns for thin slots of various lengths.

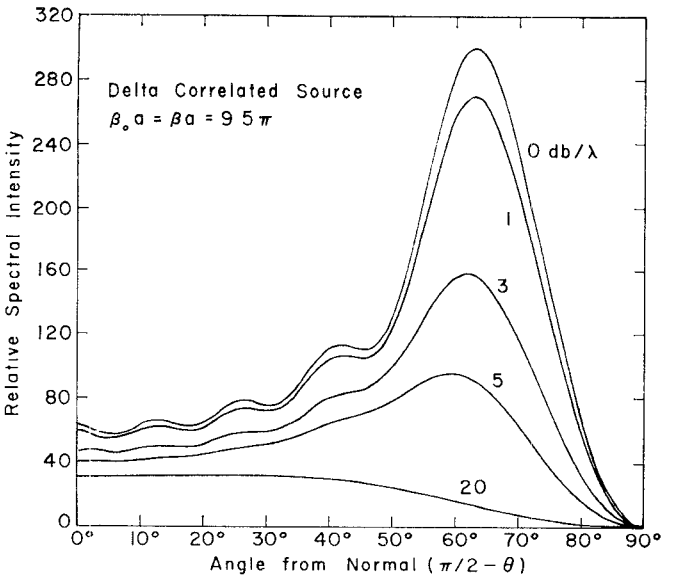

Fig. 5—Thermal radiation patterns with lossy propagation along the slot.

with the best present-day receiver this measurement is practical using silicon carbide or a similar material, but not using tungsten. However, near-zone measurements of the microwave radiation from incandescent tungsten are practical; and in fact, such a measurement has been described by Westberg [12]. A theoretical analysis of the near-zone case has not appeared in the literature.

The other experiment of interest is the measurement of the thermal radiation from a noise-excited thin slot. For this latter experiment, using a gaseous discharge as a source, one finds, as detailed below, that a receiver sensitivity of 1°K or 2°K is sufficient to permit pattern measurements in the far-zone. This sensitivity is considerably less than is quoted above for the experiments using a hot-wire source. This is due both to the much higher radiation temperature and to the higher emissivity of the gaseous discharge source.

A. Description of the Measurement

From a conceptual point of view, the measurement of a radiation pattern is quite simple. Briefly, a receiver and a transmitter are positioned at some fixed separation. For either antenna, the radiation pattern is simply the received signal as a function of the angular position as the antenna being measured is rotated about its center.

In these experiments, the transmitting antenna is typically a 4.75 by 0.122 wavelength slot in a 28 by 19 wavelength metallic ground plane. The source of the thermal radiation is an argon glow discharge tube[2] clamped to the ground plane and running along the length of the slot. This entire ground plane assembly is mounted on a wooden turntable with provisions for measuring the angle of rotation.

The receiving aperture is a microwave horn which is positioned at a 1.500-meter range with the electric-field polarization perpendicular to the long edge of the radiating slot, *i.e.*, placed at (1.500, θ, $\pi/2$) to read $E_\phi(\theta)$ in Fig. 1. The E- and H-plane dimensions of this aperture are 8.04 cm and 11.10 cm, respectively; and at 9200 Mc the *measured* absolute gain is 72 (vs a theoretical value of 70). Hence, the effective solid angle, computed from $\Omega = G\lambda^2/(4\pi r_0^2)$, is 2.70×10^{-3} sterad. Approximate criteria for the Fraunhofer region require that $r_0 > 2al/\lambda$ and $r_0 > a^2/\lambda$, in which l is the H-plane dimension of the receiving aperture [11], [14]. For $\beta_0 a = 9.5\pi$ and a frequency of 9200 Mc, these give $r_0 > 1.05$ meters and 0.74 meter, respectively. Therefore, one concludes that with a slot length of 9.5π radians, a range of 1.500 meters places the receiving aperture in the far-zone region.

The problem of detecting the thermal radiation from either a heated wire or a noise-excited thin slot is similar to a detection problem which is encountered in radio astronomy. In these two applications both the signal and the internal receiver noise have essentially the same wide spectral density. Dicke devised a practical method for detecting such signals, even though they are less than 1/1000th of the level of the receiver noise [15]. A receiver of this basic type was designed for the experiments which are described in this paper. The characteristics of this receiver are briefly summarized as follows: a total fluctuation, drift, and reflection error of 0.3 rms°K; an amplification bandwidth of 16 Mc centered at 9200 Mc (9166 to 9174 Mc and 9226 to 9234 Mc); a noise ratio for the mixer and the IF amplifier of 5 (7 db); a modulation frequency of 1000 cps; and an integration time of 30 seconds. This receiver is calibrated by using an argon noise source and a variable

[2] The dimensions of the tube are 0.765-cm ID, 0.953 cm OD, and 21.2-cm long. The tube is filled with pure argon; and for these experiments, unless otherwise specified, a pressure of 30.0 ±0.3-mm Hg and an operating point of 200 ma and 71 v are used. For these values, the kinetic temperature of the plasma electrons is computed from (8.36) of von Engel [13], and the result is a temperature

$$T = 11{,}300^\circ \text{ K}.$$

The measured value of the microwave noise temperature is, as expected [2], [4], essentially the same, *i.e.*,

$$T = 10{,}072 \pm 200^\circ \text{ K}.$$

attenuator as a secondary standard. Although these measurements are reproducible to better than 3 per cent their absolute accuracy is probably no better than 20 per cent.

B. Measurements

Experimental thermal radiation patterns are shown for slot lengths of $\beta_0 a = 7.30\pi$ and 9.50π, and for a common slot width of $\beta_0 b = 0.244\pi$ (Figs. 6, 7). The radiation received from the noise-excited thin slot is expressed in terms of an effective received temperature and this is plotted vs the angle from the normal, $\pi/2 - \theta$. In the notation of Section II, the received temperature is given by solving $kT_a df = P_{f\Omega}\Omega df$ for T_a, *i.e.*, $T_a = P_{f\Omega}\Omega/k$. Only one quadrant of the pattern is plotted due to the symmetry about the plane $\theta = \pi/2$. It should be noted that the effective received temperature, as defined above, represents only the thermal radiation from the aperture system, while the thermal radiations which are received from the other surroundings have been eliminated in the course of the data reduction.

In addition, the thermal radiation is measured for several argon-filled tubes at different pressures (Fig. 8). In this measurement there is no ground plane; but the receiver, the range, and the tube envelope are unchanged. Only the received temperature which is due to the ϕ component of the noise electric field is shown. However, in the absence of the ground plane, there is also a θ component of the electric field with a Poynting vector at $\theta = \pi/2$ of approximately one-half the value of that shown. In the presence of the ground plane, this component is no longer detected in the radiation field, due to the inefficient excitation of $E_z(x, o, z, \omega)$ when the slot is thin, *i.e.*, when $b \ll \lambda$.

In order to permit a comparison of the classical radiation pattern to those above, an experimental curve is also shown for the radiation pattern of the thin slot at optical frequencies (Fig. 9). Essentially the same experimental arrangement is preserved, except that now a sensitive photocell receiver is used to measure the intensity. The thin slot is of the order of 10^6 wavelengths long at the peak of the spectral response of the photocell.

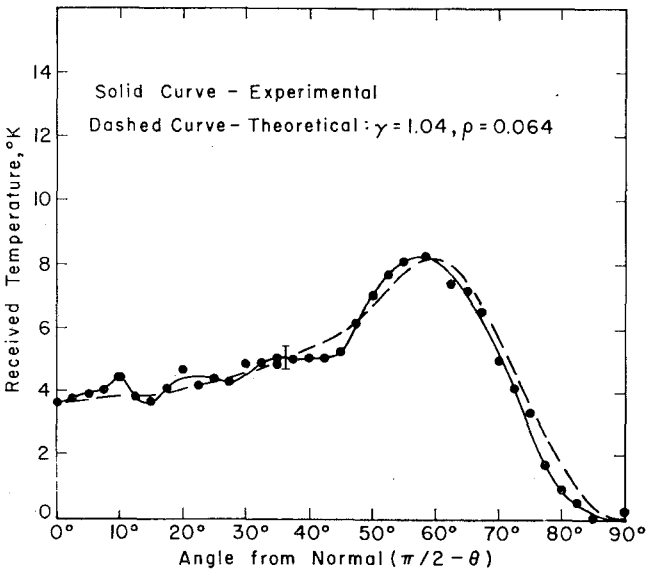

Fig. 6—Thermal radiation pattern for a thin slot of 7.3π radians in length. Data are taken for $r_0 = 1.500$ meters, $f = 9200$ Mc, and $\Omega = 2.7 \times 10^{-3}$ sterad.

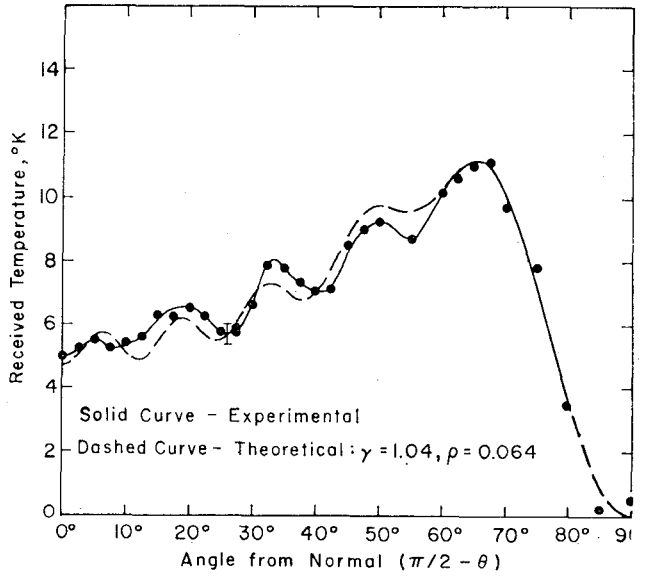

Fig. 7—Thermal radiation pattern for a thin slot of 9.5π radians in length. Data are taken for $r_0 = 1.500$ meters, $f = 9200$ Mc, and $\Omega = 2.7 \times 10^{-3}$ sterad.

C. Comparison of Measurement with Theory

First, it is seen that the optical radiation pattern is approximately Lambertian, while the microwave pattern is not. Furthermore, the general features of the microwave pattern measurements agree quite well with the theory which is presented in this paper.

In making a quantitative comparison, it is noted from a computation of (20) for the $\beta = \beta_0$ case, that there are 7 and 9 relative maxima predicted for slots of 7.3π and 9.5π radians in length, respectively. However, from the experimental curves, it is seen that there are 8 and 10 relative maxima observed in these respective cases. Although the geometry makes an exact solution difficult, it is known that the effect of the glass walls of the discharge tube is to decrease the phase velocity along the slot, while that of the plasma column itself is to increase this velocity. Apparently, their combined effect is to slightly decrease the value of the phase velocity from that in free space. Using a phase factor of $\gamma = 1.04$ and an attenuation constant of $\rho = 0.064$ (3.5 db/λ) in (20), one finds fair agreement between the experiment and the theory as is seen by comparing the solid to the dashed curve in Figs. 6 and 7. The values for γ and ρ have

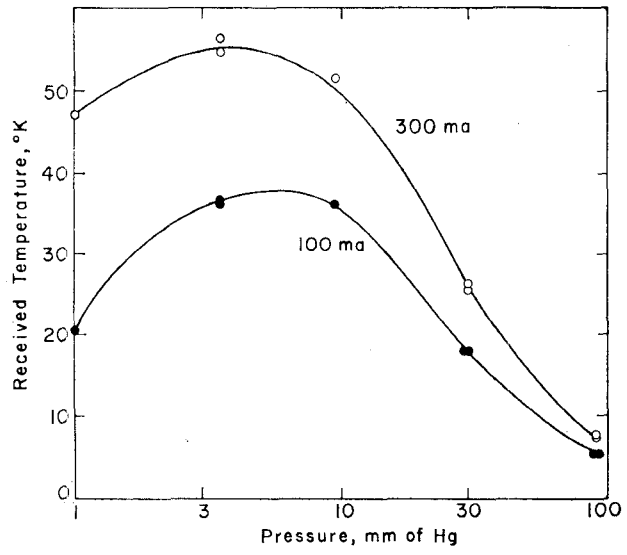

Fig. 8—Radiation level as a function of pressure for argon. Data are taken for $r_0=1.500$ meters, $f=9200$ Mc, $\theta=\pi/2$, $\Omega=2.7\times10^{-3}$ sterad and no slotted metallic plane.

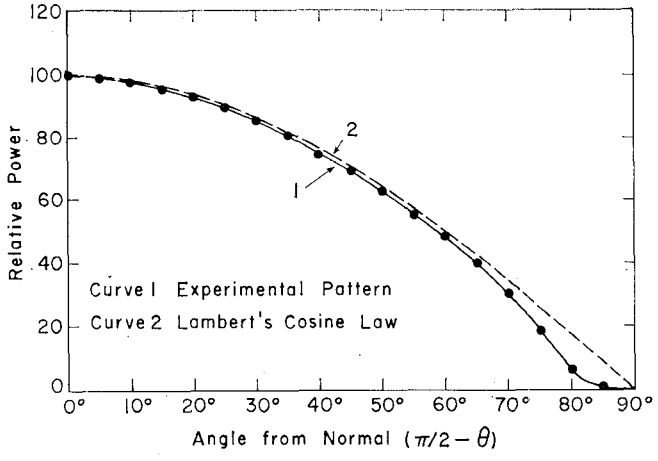

Fig. 9—Radiation pattern at optical frequencies with the same slot as in Fig. 7.

been selected to give a compromise fit for both of the slot lengths. The main discrepancy appears in the $\beta_0 a=7.3\pi$ case, where the observed ripple exceeds the theoretical value. This could be due to the compromise method of selecting γ, ρ or to some more fundamental cause, *e.g.*, a slight degree of coherence in the slot excitation.[3] The angles at which the relative maxima occur are tabulated (see Table I). In compiling this table, a lower attenuation constant is used for the $\beta_0 a=7.3\pi$ case in order to enhance the ripple and thereby to permit the determination of the tabulated angles.

[3] The radiation patterns for an exponentially-correlated source show the same general features as those given by (20), but the relative ripple is higher even for a correlation length which is less than λ [11].

TABLE I

Comparison of Experiment to Theory for the Thin Slot

Radian Length ($\beta_0 a$)		Angle of Rel. Max. $\lvert\pi/2-\theta\rvert$	z_{in} (ohms)	T_a at $\theta=\pi/2$ (°K)
7.3π	Expt.	10,21,36,58		3.6
	Theory	8,26,44,62	332.	$1.89\times10^4\sigma\delta$
9.5π	Expt.	5,19,33,50,65		5.0
	Theory	6,19,33,51,65	343.	$2.74\times10^4\sigma\delta$

The theoretical curves in Figs. 6 and 7 are drawn with an arbitrary normalization of the amplitude. Although the precise value of $\sigma\delta$ is not known, it is worth while to compare the ratio of the received temperature for the two slots at some convenient angle. Substituting the values $\beta_0 a=7.3\pi$ or 9.5π, $f=9.2\times10^9$ cps, $b=3.97\times10^{-3}$ meters, $\gamma=1.04$, $\rho=0.0641$, and $\theta=\pi/2$, one finds from (20) that $K_2=42.92$ or 66.55 and from formulas in Schelkunoff [7] that $\lvert z_{in}\rvert=332$ or 343 ohm. Then, since $T=10.1\times10^8$°K and $\Omega=2.7\times10^{-3}$ sterad, the received temperatures can be computed as $T_a=1.89\times10^4\sigma\delta$ and $2.74\times10^4\sigma\delta$ for the 7.3π and the 9.5π radian lengths, respectively. Their ratio of 0.69 agrees fairly well with the observed ratio of 0.72. From these data, an average value of $\sigma\delta$ is computed, *i.e.*, $\sigma\delta\approx1.87\times10^{-4}$ mho.

IV. Conclusions

An investigation has been made of the spatial distribution of the radiant energy emitted by a body for wavelengths at which the body dimensions and the wavelength are of the same order of magnitude. It is shown both theoretically and experimentally that in such cases the radiation pattern has the following characteristics:

1) It exhibits pronounced minima and maxima.
2) It is sensitive to the radian dimensions of the body.
3) It can have a well-defined polarization.
4) It is not, in general, a maximum in the direction for which the radiator subtends the maximum solid angle.

Although the source excitation is uncorrelated in time and in space, the *resultant* distribution of the electric field in the aperture is partially correlated, as may be shown by combining (6) and (11). It is this correlation which gives rise to the interference phenomenon in the radiated field. Furthermore, it is clear from the theory that an analogous interference effect will occur in the case of the radiation from a small hole

of arbitrary shape in an otherwise isothermal cavity. In more general terms, these effects will occur in the radiation from a blackbody surface at wavelengths which are of the order of the body dimensions.

Finally, it is worth while to recall that simply by invoking the thermodynamic principle of the detailed balancing of radiation one can compute the spectral absorptivity of a body from its spectral thermal radiation pattern or vice versa. Thus, it follows that the spectral absorptivity of a body also exhibits the above-itemized characteristics at wavelengths which are of the order of the body dimensions.

V. Acknowledgment

The author wishes to acknowledge the many helpful discussions with C. H. Papas throughout the course of this work. Valuable consultation was also given by G. J. Stanley on radiometer principles and practices during the design of the equipment for the experiments.

The author wishes to express his appreciation to R. L. Roderick and G. F. Smith who encouraged this work. This research was supported in part by a fellowship grant from the Hughes Aircraft Company, Culver City, Calif.

References

[1] H. Nyquist, "Thermal agitation of electric charge in conductors," *Phys. Rev.*, vol. 32, pp. 110–113; July, 1928.
[2] P. Parzen and L. Goldstein, "Current fluctuations in dc gas discharge plasma," *Phys. Rev.*, vol. 79, pp. 190–191; July, 1950.
[3] J. B. Johnson, "Thermal agitation of electricity in conductors," *Phys. Rev.*, vol. 32, pp. 97–109; July, 1928.
[4] W. W. Mumford, "A broad-band microwave noise source," *Bell Syst. Tech. J.*, vol. 28, pp. 608–618; October, 1949.
[5] M. A. Leontovich and S. M. Rytov, *Zh. Eksp. Teor. Fiz.*, vol. 23, pp. 246–252; 1952.
[6] H. G. Booker, "Slot aerials and their relation to complementary wire aerials," *J. IEE*, vol. 93, pp. 620–626; 1946.
[7] S. A. Schelkunoff and H. T. Friss, "Antennas, Theory and Practice," John Wiley and Sons, Inc., New York, N. Y.; 1952.
[8] J. Weber, "Scattering of electromagnetic waves by wires and plates," Proc. IRE, vol. 43, pp. 82–89; January, 1955.
[9] W. R. Smythe, "Static and Dynamic Electricity," McGraw-Hill Book Co., Inc., New York, N. Y.; 1950.
[10] M. L. Levin and S. M. Rytov, "Thermal radiation from a thin rectilinear antenna," *J. Tech. Phys.*, vol. 25, pp. 323–332; 1955.
[11] N. George, "Spatial distribution of thermal radiation at microwave frequencies," Antenna Lab., Calif. Inst. Tech., Pasadena, Calif., rept. no. 18, 1959.
[12] V. Westberg, "Measurements of noise radiation at 10 cm from glow lamps," *Chalmers Tek. Hogskol. Handl.*, nr. 180, pp. 1–14; 1956.
[13] A. von Engel, "Ionized Gases," Oxford Univ. Press, London, Eng.; 1955.
[14] S. Silver, "Microwave Antenna Theory and Design," McGraw-Hill Book Co., Inc., New York, N. Y.; 1949.
[15] R. H. Dicke, "Measurement of thermal radiation at microwave frequencies," *Rev. Sci. Instr.*, vol. 17, pp. 268–275; July, 1946.

Variational Principles and Mode Coupling in Periodic Structures*

T. J. GOBLICK, JR.† and R. M. BEVENSEE‡, member, ire

Summary—**Variational techniques are used in analyzing periodic "cold" microwave structures for the angular frequency, ω, as a function of assumed phase shift per periodic cell. Two variational expressions are given: one for ω in terms of the *E*- and *H*-fields, and one for $k^2=\omega^2\mu\epsilon$ in terms of the *E*-field. For structures with relatively light coupling between cells, the trial fields to be used with the variational expressions are composed of closed cavity modes, phase shifted by ϕ radians from cell to cell. Both variational expressions yield determinantal equations for $k^2(\phi)$ which agree with equations previously derived from a mode coupling point of view. One form of an equivalent lumped circuit is given to represent the structure within one of its pass bands.**

Curves compare the variational-mode coupling expression for $k^2(\phi)$ of a periodically lumped loaded transmission line with exact expressions.

* Received by the PGMTT, November 9, 1959; revised manuscript received, May 23, 1960. This work was supported in part by the U. S. Army Signal Corps, the U. S. Air Force Office of Scientific Res., Air Res. and Dev. Command, and the U. S. Navy Office of Naval Research.

† Dept. of Electrical Engrg., Res. Lab. of Electronics, Mass. Inst. Tech., Cambridge, Mass.

‡ Res. Div., Varian Associates, Palo Alto, Calif. Formerly with Dept. of Electrical Engrg. and Res. Lab. of Electronics, Mass. Inst. Tech., Cambridge, Mass.

I. Introduction

PERIODIC structures have received extensive theoretical and experimental treatment in the past in regard to applications in traveling wave tubes. The advent of high power traveling wave tubes proved it was still not a simple matter to design slow wave structures which could dissipate large amounts of power while still operating over a relatively large band of frequencies [1].

To analyze a simple periodic structure, such as an iris-loaded waveguide, is a formidable task. The method of analysis used here is that of mode coupling. For the case of a very heavily shunt-loaded waveguide, the coupling holes in the irises are small compared to the total iris area. The structure resembles a chain of loosely-coupled resonant cavities and so the electric and magnetic fields of the structure resemble normal cavity modes of a section of the structure. The weaker the coupling between sections is made, the closer is the resemblance of the fields to those of the actual cavities.